


Research Article

MiR-33a is a therapeutic target in SPG4-related hereditary spastic paraplegia human neurons

Fumiko Nakazeki^{1,*}, Itaru Tsuge^{2,3,*}, Takahiro Horie¹, Keiko Imamura^{2,4,5}, Kayoko Tsukita^{2,4}, Akitsu Hotta², Osamu Baba¹, Yasuhide Kuwabara¹, Tomohiro Nishino¹, Tetsushi Nakao¹, Masataka Nishiga¹, Hitoo Nishi¹, Yasuhiro Nakashima¹, Yuya Ide¹, Satoshi Koyama¹, Masahiro Kimura¹, Shuhei Tsuji¹, Motoko Naitoh³, Shigehiko Suzuki³, Yuishin Izumi⁶, Toshitaka Kawarai⁶, Ryuji Kaji⁶, Takeshi Kimura¹, Haruhisa Inoue^{2,4,5} and  Koh Ono¹

¹Department of Cardiovascular Medicine, Graduate School of Medicine, Kyoto University, Kyoto, Japan; ²Center for iPS Cell Research and Application (CiRA), Kyoto University, Kyoto, Japan; ³Department of Plastic and Reconstructive Surgery, Graduate School of Medicine, Kyoto University, Kyoto, Japan; ⁴iPSC-based Drug Discovery and Development Team, RIKEN BioResource Center (RIKEN BRC), Kyoto, Japan; ⁵Medical-risk Avoidance based on iPS Cells Team, RIKEN Center for Advanced Intelligence Project (RIKEN AIP), Kyoto, Japan; ⁶Department of Clinical Neuroscience, Institute of Biomedical Sciences, Tokushima University Graduate School, Tokushima, Japan

Correspondence: Koh Ono (kohono@kuhp.kyoto-u.ac.jp) or Haruhisa Inoue (haruhisa@cira.kyoto-u.ac.jp)



Recent reports, including ours, have indicated that microRNA (miR)-33 located within the intron of sterol regulatory element binding protein (SREBP) 2 controls cholesterol homeostasis and can be a potential therapeutic target for the treatment of atherosclerosis. Here, we show that *SPAST*, which encodes a microtubule-severing protein called SPASTIN, was a novel target gene of *miR-33* in human. Actually, the miR-33 binding site in the *SPAST* 3'-UTR is conserved not in mice but in mid to large mammals, and it is impossible to clarify the role of *miR-33* on *SPAST* in mice. We demonstrated that inhibition of *miR-33a*, a major form of *miR-33* in human neurons, via locked nucleic acid (LNA)-anti-miR ameliorated the pathological phenotype in hereditary spastic paraplegia (HSP)-SPG4 patient induced pluripotent stem cell (iPSC)-derived cortical neurons. Thus, miR-33a can be a potential therapeutic target for the treatment of HSP-SPG4.

Introduction

MicroRNAs (miRNAs; miRs) are small non-protein-coding RNAs that bind to specific mRNAs and inhibit translation or promote mRNA degradation. MiRNAs show cell-type-, tissue-, and species-specific regulation of their targets in different cellular contexts [1,2]. Therefore, it is critical to study miRNA function in appropriate cell-types, tissues, and species. Previously, we demonstrated that *miR-33* controls lipid homeostasis with the use of *miR-33*-deficient mice [3]. However, the physiological functions of *miR-33* in humans are still unknown because of a lack of appropriate models.

MiR-33 has two isoforms, *miR-33a* and *miR-33b*. Although *miR-33a* and *b* differ by only two nucleotides in their mature forms, they are identical in their seed sequence. *MiR-33a* has been highly conserved throughout evolution, whereas *miR-33b* is present only in the sterol regulatory element binding factor (SREBF) 1 gene of large mammals, and rodents lack *miR-33b* [3–6]. To investigate novel target genes of *miR-33a/b* in human, we generated *miR-33*-single (*miR-33a* or *miR-33b*) and -double (*miR-33a* and *miR-33b*) knockouts (KO) in human induced pluripotent stem cells (iPSCs) by clustered regularly interspaced short palindromic repeat (CRISPR)-Cas9 technology, and analyzed their transcriptome.

In the current study, we revealed that *SPAST* was a novel target gene of *miR-33* in human. Actually, the *miR-33* binding site in the *SPAST* 3'-UTR is conserved not in mice but in mid to large mammals, and it is impossible to clarify the role of *miR-33a* and *miR-33b* on *SPAST* in mice. *SPAST* encodes a microtubule-severing protein called SPASTIN [7–9], and mutations in the *SPAST* gene (previously known as *SPG4*) are the most common causes of hereditary spastic paraplegia (HSP-SPG4) [10–12]. We

* These authors contributed equally to this work.

Received: 08 November 2018

Revised: 13 February 2019

Accepted: 18 February 2019

Accepted Manuscript Online:
18 February 2019

Version of Record published:
22 February 2019

demonstrated that *miR-33a* affected the pathological phenotypes though regulating *SPAST* expression in SPG4 patient iPSC-derived cortical neurons. Moreover, inhibition of *miR-33a*, a major form of *miR-33* in human neurons, via locked nucleic acid (LNA)-anti-miR ameliorated the pathological phenotype in HSP-SPG4 patient neurons. Thus, *miR-33a* can be a potential therapeutic target for the treatment of HSP-SPG4.

Material and methods

Generation of iPSCs and cell culture

SPG4 patient iPSCs were generated from peripheral blood mononuclear cells (PBMCs) or T-lymphocytes using episomal vectors for OCT3/4, Sox2, Klf4, L-Myc, Lin28, and dominant negative p53 or OCT3/4, Sox2, Klf4, L-Myc, Lin28, and p53-shRNA, as reported previously [39], and were cultured on an SNL feeder layer with human iPSC medium (primate embryonic stem cell medium; ReproCELL, Yokohama, Japan) supplemented with 4 ng/ml basic fibroblast growth factor (FGF; Wako Chemicals, Osaka, Japan) and penicillin/streptomycin. The present study and the use of hiPSCs were approved by the Ethics Committee of Kyoto University, and informed consent was obtained from all donor subjects from which hiPSC lines were generated in accordance with the Declaration of Helsinki. All methods were performed in accordance with the relevant guidelines and regulations.

Construction of plasmids for gene targeting

For CRISPR-Cas9n plasmids, guide RNAs were designed using CRISPR Design (<http://crispr.mit.edu/>). The guide RNA oligonucleotides (Supplementary Table S1) were inserted into a pHL-Ha-ccdB plasmid. For constructing the donor plasmid, we modified pBluescript SK (+) by inserting the selection cassette and the fragments of genomic sequences 5' and 3' amplified by PCR. Each homologous arm was bound using an In-Fusion HD cloning kit (Clontech, Mountain View, CA) as 5' and 3' homology arms.

Genome edition of iPSCs by gene targeting

For transfection of CRISPR-Cas9n, 1×10^6 iPSCs were electroporated with 3 μ g each of two gRNA plasmids, 5 μ g of Cas9n (D10A Cas9) plasmid, and 10 μ g of donor plasmid by using the NEPA21 electroporator (Nepa Gene, Chiba, Japan). Transfected cells were plated onto feeder cells and cultured in human ES medium supplemented with 10 μ M of Y-27632 for 1 day. Three days after transfection, neomycin and/or puromycin selection was applied and continued for 10 days. Resistant colonies were picked out and expanded for genomic DNA extraction and PCR screening. To remove the selection cassette, cells were transiently transfected with a Cre-recombinase expressing plasmid (pCXW-Cre-Puro) by electroporation and puromycin-resistant colonies were selected. Selection cassette excision and bi-allelic deletion for *miR-33a* and/or *miR-33b* were confirmed by genomic PCR screening and Sanger sequence analysis.

Induction of cortical neuron differentiation

Human iPSCs were dissociated into single cells and quickly reaggregated in U-bottomed 96-well plates for suspension culture (Greiner Bio-One, Frick-enhausen, Germany), pre-coated with 2% Pluronic (Sigma-Aldrich, St. Louis, MO) in 100% ethanol. Aggregations of embryoid bodies (EBs) were cultured in 5% DFK medium (Dulbecco's modified Eagle's medium/Ham's F12 (Sigma-Aldrich), 5% KSR (Gibco, Waltham, MA), NEAA (Invitrogen), L-glutamine (Sigma-Aldrich), 0.1 M 2-mercaptoethanol (Invitrogen) with or without 2 μ M dorsomorphin and 10 μ M SB431542 (Wako Chemicals) in a neural inductive stage (days 0–8). After induction, EBs were transferred onto Matrigel (Becton Dickinson)-coated 6-well culture plates and cultured in supplemented with $1 \times N2$ supplement (Invitrogen), 2 μ M dorsomorphin, and 10 μ M SB431542 in the patterning stage (days 8–24). After patterning stage, migrated neural precursor cells were separated from the plate bottom using Accutase (Innovative Cell Technologies, Inc.) and cultured in Neurobasal medium FULL, Neurobasal medium (Invitrogen/Gibco) supplemented with $1 \times B27$ without Vitamin A (Invitrogen/Gibco), $1 \times$ Glutamax (Invitrogen/Gibco), 10 ng/ml BDNF, 10 ng/ml GDNF, and 10 ng/ml NT-3 on Matrigel-coated 12-well or 24-well culture plates or cover slips in the neural maturation stage and then cultured until used for experiments.

Western blotting

Western blotting was performed using standard procedures as described previously [40]. Samples were lysed in lysis buffer consisting of 100 mM Tris-HCl, pH 7.4, 75 mM NaCl, and 1% Triton X-100 (Nacalai Tesque). The lysis buffer was supplemented with complete mini protease inhibitor (Roche), ALLN (25 μ g/ml), 0.5 mM NaF, and 10 mM Na_3VO_4 just before use. The protein concentration was determined using a bicinchoninic acid (BCA) protein

assay kit (Bio-Rad). All samples (10 µg of protein) were suspended in lysis buffer, fractionated using NuPAGE 4–12% Bis-Tris (Invitrogen) gels and transferred onto a Protran nitrocellulose transfer membrane (Whatman). The membrane was blocked using 1 × phosphate-buffered saline (PBS) containing 5% non-fat milk for 1 h and incubated with primary antibodies against SPASTIN (S7074, Sigma–Aldrich), ABCA1 (NB400-105, Novus Biologicals), sterol regulatory element binding protein (SREBP) 1 (2A4, Santa Cruz), SREBP-2 (Cayman), TF2B (EP4588, Abcam), or β-actin (C4, Santa Cruz) overnight at 4°C. After a washing step in PBS-0.05% Tween 20 (0.05% T-PBS), the membrane was incubated with the secondary antibody (anti-rabbit or anti-mouse IgG HRP-linked; 1: 2000) for 1 h at room temperature. The membrane was then washed in 0.05% T-PBS and detected by ECL Western Blotting Detection Reagent (GE Healthcare), using an LAS-4000 system (GE Healthcare Life Science).

RNA extraction and qPT-PCR

Total RNA was isolated and purified using TriPure Isolation Reagent (Roche), and cDNA was synthesized from 100 ng of total RNA using a Transcriptor First Strand cDNA Synthesis Kit (Roche) in accordance with the manufacturer's instructions. For quantitative RT-PCR, specific genes were amplified by 40 cycles using SYBR Green PCR Master Mix (Applied Biosystems). Expression was normalized to the housekeeping gene 18S ribosomal RNA. Gene-specific primers are listed in Supplementary Table S2.

Quantitative PCR for miRNAs

Total RNA was isolated using TriPure Isolation Reagent (Roche). *MiR-33* was measured in accordance with the TaqMan MicroRNA assays (Applied Biosystems) protocol, and the products were analyzed using a thermal cycler (ABI Prism7900HT sequence detection system). Samples were normalized by U6 snRNA expression. We also measured 16, 4, 1 pM, 250, 62.5, and 15.625 fM oligonucleotide of *miR-33a* and *miR-33b*, and created a calibration curve. We calculated the absorbance value of samples from the figure to determine its concentration.

Dual luciferase assays

Full length PCR fragments of the 3'-UTR of *SPAST* were amplified from human iPSC cDNAs and subcloned in psi-CHECK2-let-7 8X vector (addgene). To create WT or mutant 3'-UTR luciferase reporter genes, a fragment of the *SPAST* 3'-UTR as follows was inserted into a psi-CHECK2-let-7 8X vector:

Wild-type: acagacttaaacaaaatatacaatgcaaatgtaattttttgtgtttaag
Mutant: acagacttaaacaaaatataccgtaaaatgtaattttttgtgtttaag

Luciferase activities were measured as described previously [41].

SPASTIN and green fluorescent protein overexpression

The human *SPAST*, with or without the full length 3'-UTR of *SPAST*, was cloned from human iPSCs into the pCMV-internal ribosome entry site (IRES)-green fluorescent protein (GFP) vector and then CMV promoter was replaced with a Synapsin I promoter which is relatively neuron-specific. We produced lentiviral stocks in 293FT cells in accordance with the manufacturer's protocol (Invitrogen). In brief, virus-containing medium was collected 48-h post-transfection and filtered through a 0.45-µm filter. Cells were infected with *SPAST*, *SPAST* with 3'-UTR, or empty GFP control lentivirus. Neural cultures were allowed to differentiate for 10 days after DNA transduction. Infected cells were highlighted with GFP.

Cell transfection with LNA-anti-*miR-33*

Cells were transfected with 10 nM LNA-anti-*miR-33* or LNA-control using Lipofectamine RNAiMAX (Invitrogen) in accordance with the manufacturer's instructions. Cells were used for analysis 48 h after transfection.

Immunocytochemistry

Cells were fixed in 4% paraformaldehyde (pH 7.4) for 30 min at room temperature and rinsed with PBS. The cells were permeabilized in PBS containing 0.2% Triton-X 100 for 10 min at room temperature, followed by rinsing with PBS. Nonspecific binding was blocked with Block Ace (DS pharma biomedical) for 60 min at room temperature. Cells were incubated with primary antibodies overnight at 4°C, and then labeled with appropriate fluorescent-tagged secondary antibodies. DAPI (DOJINDO) was used to label nuclei. The following primary antibodies were used in

immunocytochemistry: β III tubulin (1:1000, CST, 5568S). For evaluating the positive count ratio of immunocytochemistry, we imaged the cells using automated microscopy by ArrayScan and counted the immunostained structures by using HCS Studio 2.0 Cell Analysis Software (Thermo Fisher Scientific).

Statistical analysis

Data are presented as means \pm standard error of the mean (S.E.M.). Statistical comparisons were performed using unpaired t-test or one-way analysis of variance (ANOVA) with Sidak's *post hoc* test (three or more groups). The statistical analysis used is indicated in each of the figure legends. A *P* value of <0.05 was considered as statistically significant. Statistical analyses were performed using GraphPad Prism 6 (GraphPad Software, Inc.).

Results

Generation of *miR-33* KO human iPSCs

To investigate the role of *miR-33* in human cells, we generated *miR-33* single KO and *miR-33* double KO cells using human iPSCs. We constructed a pair of CRISPR guide RNA (gRNA) expression vectors (Supplementary Table S1), and co-electroporated them into control iPSCs (named 201B7) together with D10A Cas9 nickase (Cas9n) to introduce a double-strand break. The double-nicking approach was chosen to minimize off-target mutagenesis. Previous studies showed that the miRNA seed region is the preferred cleavage site to KO miRNA genes with high efficiency and specificity, we triggered PAMs (NGG) within/adjacent to each seed region [13,14]. To facilitate the screening for bi-allelic deletion, we combined the above procedure with homologous recombination donor vectors, which enabled neomycin- and/or puromycin-resistant cell selection (Supplementary Figure S1a). The predicted sizes of indels, such as mature *miR-33* sequence deletion and loxP sequence insertion, were identified by DNA sequencing (Figure 1A, Supplementary Figure S1b). Complete loss of *miR-33a/b* expression in KO iPSCs was confirmed by RT-PCR analysis (Figure 1B) although slight signals remained because of the PCR-based miRNA measurement. Deletion of *miR-33a* and/or *miR-33b*, encoded by an intron of *SREBF2* and *SREBF1*, did not affect the protein levels of their host genes or splicing (Figure 1C,D). We further attempted to confirm whether the deletion of *miR-33* was established without interfering with the activation of their host genes. NK104, an HMG-CoA inhibitor, activates the transcription of *SREBF2* and TO90137, an LXR agonist, enhances *SREBF1* expression. *SREBF2* and *SREBF1* mRNAs in control and KO iPSCs were significantly increased with these pharmacological stimulations, and expression levels of *miR-33a/b* in control iPSCs increased in parallel. Because the expression levels of *miR-33a* and/or *miR-33b* in each KO iPSCs were undetectable even with the stimulation of their host genes, complete loss of *miR-33a* and/or *miR-33b* was achieved in *miR-33*-single and -double KO iPSCs (Supplementary Figure S1c,d). Chromosomal Q-band analyses showed that our established iPSC lines had normal karyotypes (Supplementary Figure S1e).

miR-33 regulates *SPAST* expression in human

To analyze the effect of *miR-33* on human cells, we performed microarray analysis using *miR-33*-single, -double KO, and control iPSCs (201B7). The microarray data detected 93 up-regulated genes and 191 down-regulated genes in *miR-33a* KO, 99 up-regulated genes and 110 down-regulated genes in *miR-33b* KO and 49 up-regulated genes and 127 down-regulated genes in *miR-33* double KO iPSCs versus control iPSCs (fold change >2) (Figure 2A). We searched for *miR-33* target genes among the up-regulated genes in all of the *miR-33*-single and -double KO iPSCs with the use of a public database, TargetScan (<http://www.targetscan.org>). As shown in Figure 2B, *SPAST* was the only gene identified by this method. Next, we validated the expression levels of *SPAST* and its translational product, SPASTIN by RT-PCR and Western blotting analysis, respectively (Figure 2C,D). The presence of two translation initiation codons in *SPAST* allowed the synthesis of two SPASTIN isoforms: a full-length isoform called M1 and a slightly shorter isoform called M87. M87 is more abundant in both neuronal and non-neuronal tissues [15–17]. The *SPAST* 3'-UTR has a potential binding site for *miR-33* in mid to large mammals. However, there is no target site in mice (Figure 2E). To test whether the putative *miR-33* target sequence in the *SPAST* 3'-UTR could mediate translational repression, we inserted the 3'-UTR of the *SPAST* transcript into a luciferase expression plasmid (psiCHECK-2-*SPAST* 3'-UTR) and transfected it into HEK 293T cells. CMV-driven *miR-33a* and *miR-33b* expression resulted in a decrease in luciferase activity compared with the control vector (miR-control; miR-C) (Figure 2F). Mutation in the potential binding site in the 3'-UTR abolished the effect of *miR-33* (Figure 2G). Moreover, reporter vector with mouse *SPAST* 3'-UTR did not respond to *miR-33a* or *miR-33b* (Supplementary Figure S2a).

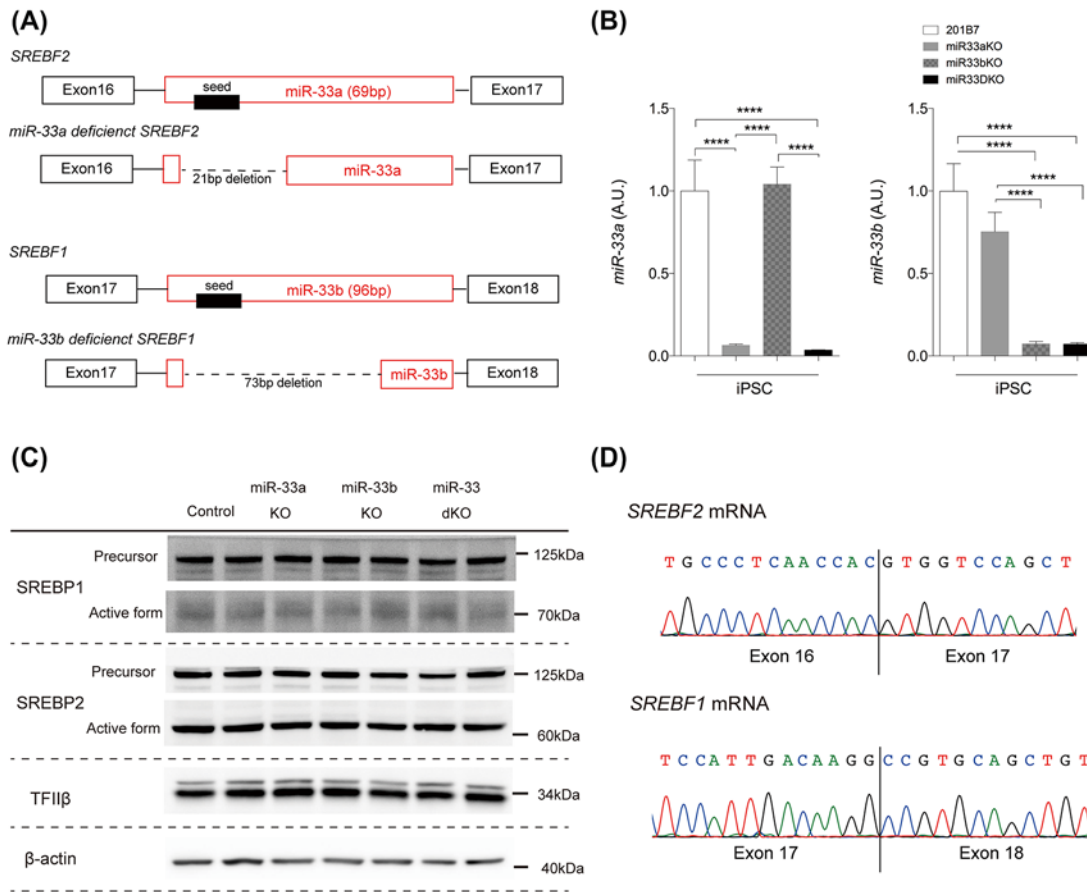


Figure 1. CRISPR-Cas9 can significantly down-regulate the expression of *miR-33*

(A) Schematic structure of the *miR-33* locus and DNA cleavage sites (B) Expression levels of mature *miR-33* were normalized using that of U6 small nuclear RNA. *n*=3 in each clone, two clones per each KO line. *****P*<0.0001 by one-way ANOVA. (C) Protein levels of host genes in *miR-33* KO iPSCs. Two clones per KO line. (D) Sequencing at the junction between exon 16 and 17 of *SREBF2* mRNA and between exon 17 and 18 of *SREBF1*, indicating correctly spliced.

Loss of SPASTIN activity is the characteristic phenotype of HSP-SPG4

Mutations in the *SPAST* gene (located on 2p22.3) are the most common causes of HSP [7–9]. Autosomal-dominant HSP-SPG4 in most cases is considered a prototypical HSP with gait impairment because of spasticity and weakness of the lower extremities [7–9]. Considering the effect of *miR-33* in the regulation of *SPAST* gene in human, we hypothesized that inhibition of *miR-33* would promote the activation of one normal *SPAST* allele and subsequently reduce the pathological phenotypes. To address this hypothesis, we generated iPSCs from one SPG4 patient and healthy controls (named hc1-A and hc3-A). The patient carried the heterozygous G>A substitution located in intron 9 of the *SPAST* gene, which alters the splice site (IVS9+1 G→A), causing skipping of exon 9. Exon 9 lies within the AAA cassette-encoding region of the gene (Pedigree in Figure 3A). This IVS9+1 G→A mutation in patients with HSP was described previously [18]. This region was sequenced to confirm that the SPG4-derived iPSCs maintained the mutation in the *SPAST* gene (Figure 3B, Supplementary Figure 2b,c). Chromosomal Q-band analyses showed that this iPSC from SPG4 had a normal karyotype (Supplementary Figure 2d). To investigate the cellular phenotype, we differentiated SPG4 and control iPSCs into cortical neurons using the quick embryoid body-like aggregate (SFEBq) method, as described previously [19]. Because SPG4 is caused by autosomal dominant mutations, SPG4 patients likely have about 50% SPASTIN activity if one allele is non-functional. A previous study revealed that neurons derived from SPG4 patients with a splice site mutation showed approximately 50% reduction in SPASTIN protein levels compared with controls [20]. Consistent with this, there was a significant decrease in both *SPAST* mRNA and SPASTIN protein levels compared with controls (Figure 3C,D). Finally, we examined SPG4-derived neurite morphology. Immunofluorescent

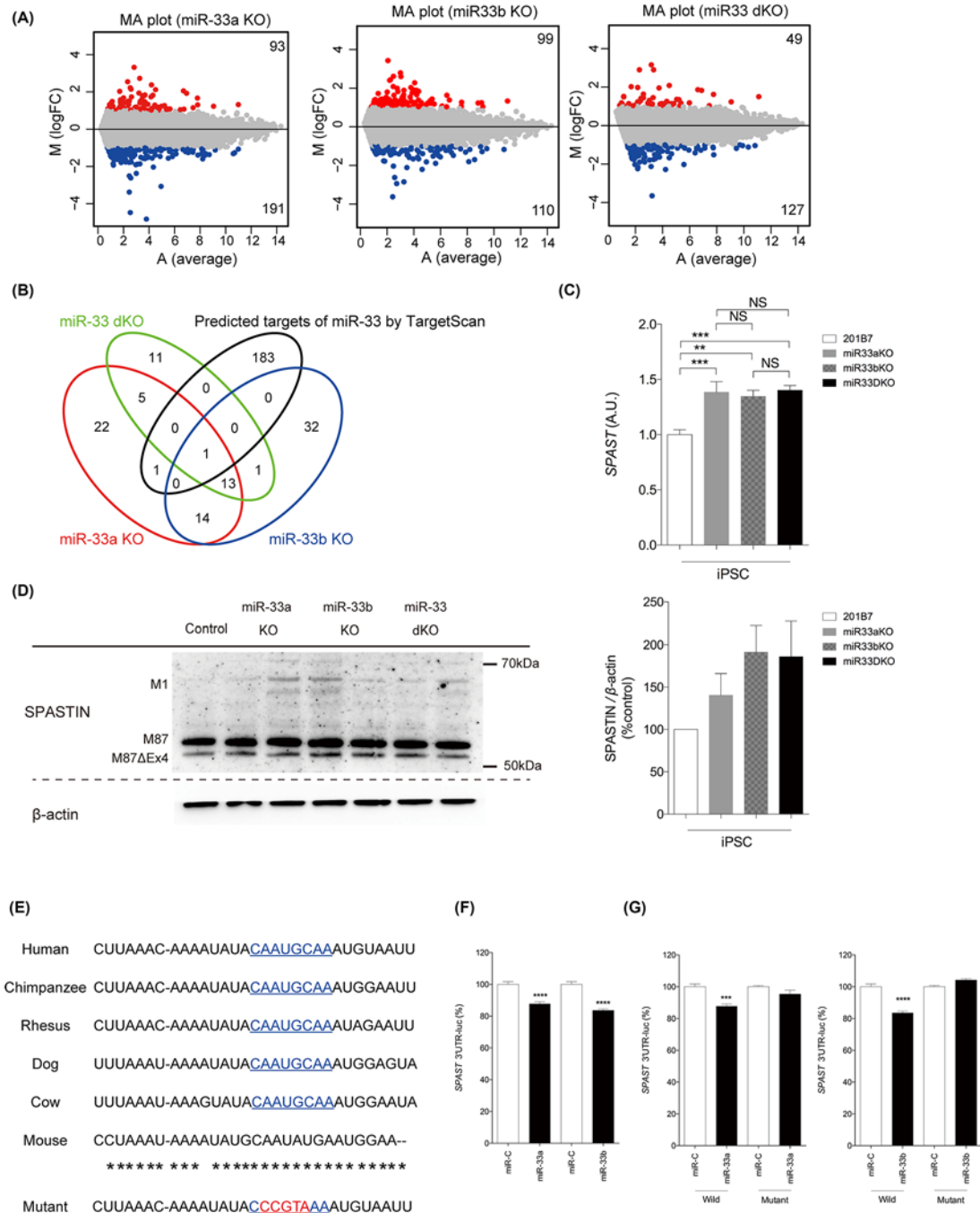


Figure 2. Expression levels of *SPAST* up-regulated in all *miR-33* KO iPSCs
(A) MA plot (M, log ratio; A, average mean) of *miR-33* KO iPSCs versus control [fold change (FC) >2 was highlighted in red and blue]. **(B)** Venn diagram displaying overlaps between up-regulated genes in each KO iPSCs and top 200 predicted targets of *miR-33* by TargetScan. **(C)** Validation of *SPAST* induced by deficiency of *miR-33*. *n*=3 in each clone, two clones per KO line. ***P*<0.01, ****P*<0.001 by one-way ANOVA. **(D)** Protein levels of *SPASTIN* in *miR-33* KO iPSCs. Two clones per KO line, two independent experiments. **(E)** Conservation of *miR-33* target regions in the 3'-UTR of *SPAST*. Underlined sequences are the potential binding site of *miR-33* seed sequences. *indicated the conservation among species. Mutant 3'-UTR sequences are highlighted in red. **(F)** 3'-UTR reporter assay used to verify the target. Luciferase reporter activity of human *SPAST* gene 3'-UTR constructs in HEK293T cells overexpressing *miR-C* and *miR-33* (*n*=6 each, *****P*<0.0001 by unpaired *t*-test). **(G)** Luciferase reporter activity of the WT or mutant *SPAST* 3'-UTR at the potential *miR-33* binding site in HEK293T cells (*n*=6 each, ****P*<0.001, *****P*<0.0001 by unpaired *t*-test).

Downloaded from <https://portlandpress.com/clinicalscience/article-pdf/133/4/583/842836/cs-2018-0980> pdf by Tokushima Daigaku - Kuramoto Chitku user on 11 August 2020

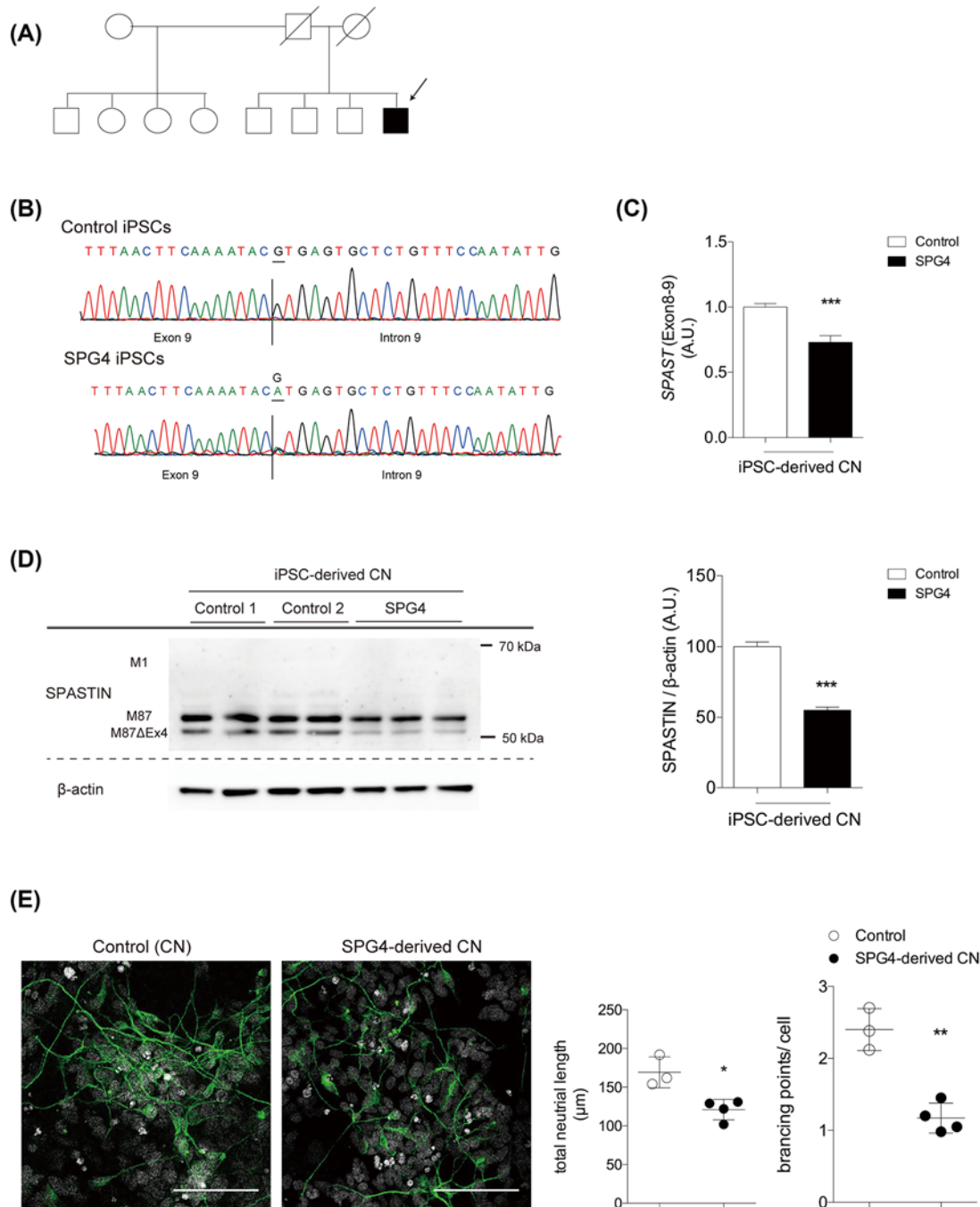


Figure 3. Characteristics of SPG4-derived cortical neurons

(A) Pedigree of SPG4 patient included in the study. (B) Sequence for the presence of the heterozygous SPG4 mutation IVS9+1G→A. (C) Expression levels of SPAST in iPSC-derived cortical neurons. $n=5$ in SPG4, $n=4-5$ each in control, two clones per control line. $***P<0.001$ by unpaired t -test. (D) Protein levels of SPASTIN in iPSC-derived cortical neurons. $n=3$ in SPG4, $n=2$ each in control. $***P<0.001$ by unpaired t -test. (E) Representative immunofluorescent staining of βIII-tubulin (green) using SP8 confocal microscope system. Nuclei are labeled with DAPI (white). Neurite length and branching points from SPG4-derived cortical neurons compared with control neurons. Images were automatically captured using the Cellomics ArrayScanVTI. Each dot indicates the mean value of 50 different microscopic fields. $*P<0.05$, $**P<0.01$ by unpaired t -test.

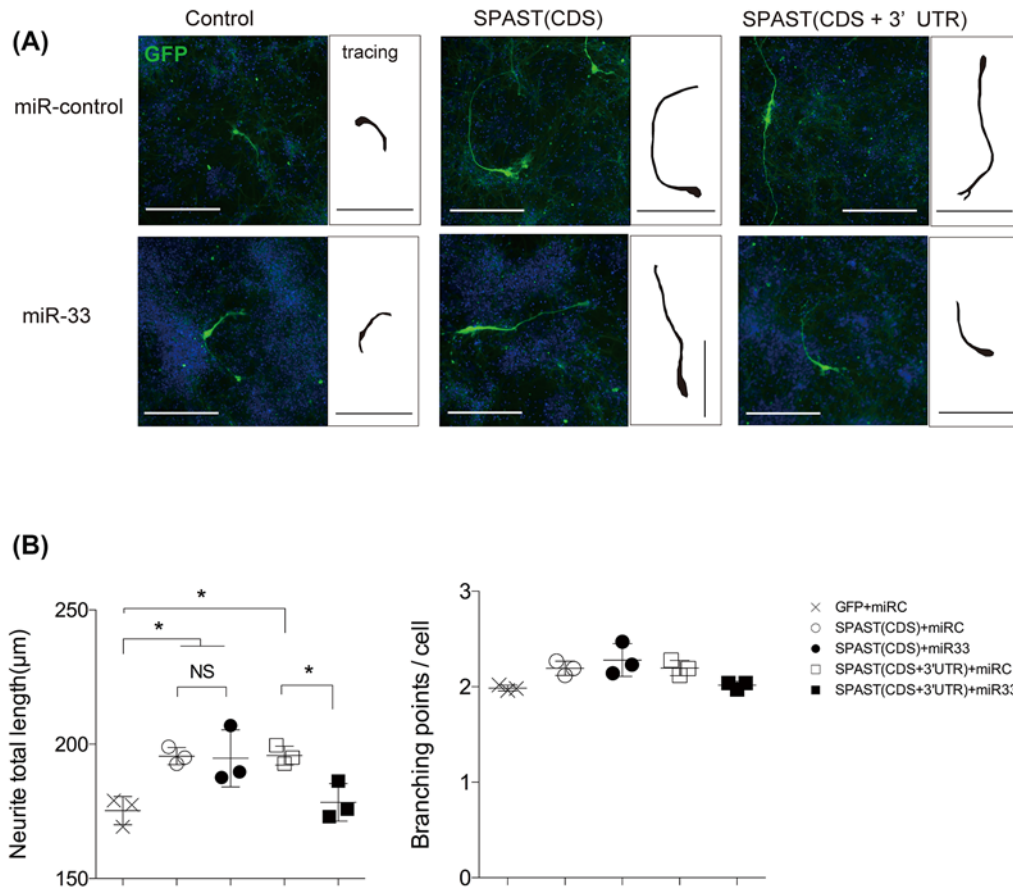


Figure 4. miR-33 affected neural phenotypes in SPG4 through modulating SPAST expression

(A) Representative images of transfected SPG4-derived neurons, labeled with GFP. Neurite tracings are shown in black insert. Scar bars: 100 μm. (B) The total neurite length and branching points in GFP⁺ SPG4-derived neurons, transfected with the indicated lentivirus. Images were automatically captured using the Cellomics ArrayScanVTI. Using a 10× objective. Each dot indicates the mean value of 50 different microscopic fields. * $P > 0.05$ by one-way ANOVA.

staining revealed that the total neurite length and the numbers of branching points were decreased in SPG4-derived cortical neurons (Figure 3E).

miR-33a decreases the neurite length of cortical neurons derived from iPSCs through SPAST 3'-UTR regulation

The previous study showed that a reduction in SPASTIN levels was directly linked with the observed disease phenotypes, and it was demonstrated that SPG4-derived neurons overexpressing SPASTIN could rescue neurite outgrowth defects [20]. To determine whether *miR-33a* directly regulates *SPAST* expression and affects neural phenotypes in SPG4-derived neurons, we co-transfected lentiviral constructs into SPG4-derived neurons. We overexpressed GFP-IRES-SPAST with/without the 3'-UTR including a potential binding site (Vector 1 and Vector 2) in the presence of synapsin I neuronal driver. We used GFP-overexpressing SPG4 neurons as a control (Supplementary Figure S3a). Consistent with previous reports [20], SPG4-derived neurons overexpressing SPASTIN restored neurite length compared with GFP-controls (Figure 4A). Co-transfected CMV-driven miR-C with overexpression of either of Vector 1 or Vector 2 led to the restoration of neurite length in SPG4-derived neurons (Figure 4A). However, co-transfection of CMV-driven *miR-33a* with Vector 2 decreased neurite lengths, which was not observed with Vector 1 (Figure 4B, Supplementary Figure S3b). We could not observe the difference in branching points (Figure 4B).

Inhibition of *miR-33a* via locked nucleic acid-anti-miR ameliorates neurite length

We demonstrated that *miR-33a* modulated neural phenotypes in SPG4-derived neurons by targetting the *SPAST* 3'-UTR. To investigate whether the inhibition of *miR-33* could be a potential therapeutic target for SPG4, SPG4-iPSCs were transfected with LNA: anti-*miR-33a*, or control (LNA: anti-miR-C) because the absolute levels of *miR-33a* were more abundant than that of *miR-33b* in both the undifferentiated state and after neural differentiation (Supplementary Figure S4a). To confirm the knockdown efficiency of the LNA-anti-*miR-33a*, the expression levels of *miR-33a* were evaluated by RT-PCR at 48-h after transfection. There was almost 40% knockdown of *miR-33a* in iPSC-derived neurons (Supplementary Figure S4b). Down-regulation of *miR-33a* was associated with up-regulation of *ABCA1*, which is known as a direct downstream target of *miR-33a* (Supplementary Figure S4c). *SPASTIN* levels were significantly increased by LNA: anti-*miR-33a* (Figure 5A). We observed that not the branching point but the neurite length in SPG4-derived neurons was significantly restored at 48-h after transfection with LNA: *miR-33a*, suggesting the therapeutic potential of *miR-33a* inhibition for the treatment of SPG4 (Figure 5B,C). We also conducted the similar experiments by the use of LNA anti-*miR-33b*. However, there was no difference in branching point or neurite length (Figure 5B,C). Moreover, enhanced expression of *miR-33a* was observed in our SPG4-derived neurons compared with the controls, in parallel with host gene mRNA expression and protein levels (Supplementary Figure S5a–c). To identify the cause of *miR-33a* elevation, we established *Spast*-knockdown Neuro 2a lines using lentiviral infection of shRNA constructs. There was about 50% knockdown of *Spast* mRNA expression in *Spast* RNAi lines 1 and 2 (Supplementary Figure S5d). RT-PCR results revealed that the neuronal cells with reduced spastin compared with the controls tended to increase the expression levels of *miR-33a* in parallel with the host gene, *Srebf2* (Supplementary Figure S5e). Thus, enhanced expression of *miR-33a* in our SPG4-derived neurons may have a direct effect in *SPASTIN* reduction.

Discussion

In previous reports, the roles of *miR-33* in mice have been explored, with evidence of its involvement in the regulation of lipid metabolism [21–23]. However, in human, the roles of *miR-33* remain unclear because of a lack of appropriate models. Here, we generated *miR-33*-single (*miR-33a* or *miR-33b*) and -double (*miR-33a* and *miR-33b*) KO iPSCs using CRISPR-Cas9 technology and demonstrated a complete deletion of mature *miR-33* biogenesis in these KO iPSCs. Furthermore, we identified that *SPAST* was a novel target gene of *miR-33* in human. *SPAST*, one of the genes responsible for HSP, was directly regulated by *miR-33*. Inhibition of *miR-33a* by LNA partly reduced the pathological phenotypes of SPG4-derived cortical neurons. It is tempting to speculate that inhibition of *miR-33a* by synthetic RNA oligonucleotides could promote the activation of one normal *SPAST* allele and subsequently reduce the pathological phenotypes.

Specific and stable KO for miRNA is essential for studying miRNA functions. Genetic KO of the miRNA under study is the most reliable technique for loss-of-function analyses. Recently, CRISPR-Cas9 technology has been applied for the study of gene functions in a variety of models. In addition, several publications reported that CRISPR-Cas9 technology could repress miRNA expression by targetting the terminal loop or 5' region of the pre-miRNA [14]. In the present study, we generated *miR-33*-single and -double KO iPSCs using CRISPR-Cas9 technology without affecting the expression of their host genes.

Neurodegenerative diseases are largely considered to be proteinopathies with alterations in the expression levels of these genes [24]. Previous studies demonstrated that SPG4-derived neurons had lower numbers of shorter and less branched primary neurites, which was similar to the phenotype observed when human ECS-derived neurons were depleted of *SPASTIN* by siRNA [25]. In addition, overexpression of *SPASTIN* in SPG4-derived neurons restored these pathological phenotypes [20], suggesting that the SPG4-phenotype is dependent on *SPASTIN* dosage. The overwhelming majority of mutations found in HSP-SPG4 patients abolished the microtubule-serving activity of *SPASTIN* generated from the mutated *SPAST* allele and theoretically resulted in the accumulation of microtubules that were lower in number but more stable [26], which led to nervous system abnormalities during development.

In the present study, we hypothesized that inhibition of *miR-33* could increase *SPASTIN* levels via promoting the transcription of one normal allele and subsequently reduce the pathological phenotypes. To address this hypothesis, we generated iPSCs from one SPG4 patient and controls. Consistent with previous studies, we observed that the SPG4-derived neurons, carrying a *SPAST* IVS9+1G→A mutation, showed impaired neurite length and branching. Moreover, we observed that co-transfected CMV-driven miR-C with overexpression of either of *SPAST* with or without the 3'-UTR including the binding site was sufficient to restore neurite length and normal branching in SPG4-derived neurons. On the other hand, co-transfected CMV-driven *miR-33a* with *SPAST* with the 3'-UTR

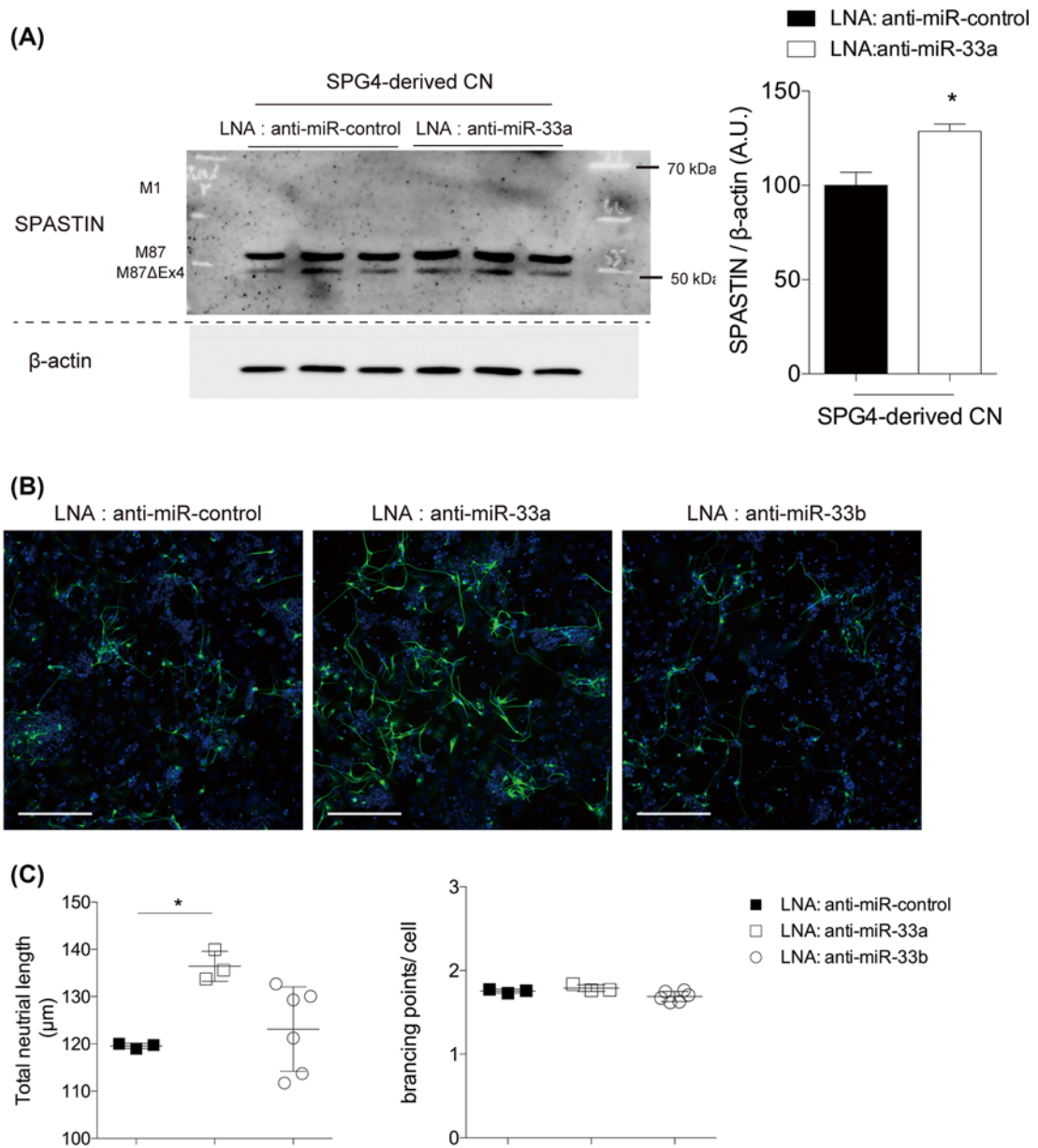


Figure 5. Inhibition of *miR-33* by LNA restored neurite length in SPG4-derived neurons

(A) Protein levels of SPASTIN in SPG4-derived neurons with LNA treatment. $n=3$ each. * $P<0.05$ by unpaired t -test. (B) Representative immunofluorescent staining of $\beta 3$ -tubulin (green). SPG4-derived neurons were treated with LNA: control, LNA: anti-*miR-33a*, or LNA: anti-*miR-33b* for 48 h. (C) The total neurite length and branching points in SPG4-derived neurons with LNA treatment. Images were automatically captured using the Cellomics ArrayScanVTI. Using a 10 \times objective. Each dot indicates the mean value of 50 different microscopic fields. * $P<0.05$ by one-way ANOVA.

impaired the restoration of the neurite phenotypes, which was not observed in the case of *SPAST* without the 3'-UTR. Our findings indicated that *miR-33a* directly regulated *SPAST* expression and affected neural phenotypes in SPG4-derived neurons.

Several siRNAs and antisense oligonucleotides with LNA are currently under investigation in clinical trials for various diseases [27]. In the current study, we demonstrated that LNA-based pharmacological inhibition of *miR-33a* restored neurite length in SPG4-derived cortical neurons. MiRNA expression profiling studies were initially done in the cancer field, and certain miRNAs, including *miR-33*, have been identified as having tumor-suppressing functions or oncogenic potential [28,29]. Recently, miRNA profile studies identified differentially expressed miRNAs in

neurodegenerative diseases, such as Alzheimer disease [30–32] and Parkinson disease [33]. We observed enhanced expression of *miR-33a* in our SPG4-derived neurons, and this may explain the substantial effect of LNA-based inhibition of *miR-33a*. HSP are mainly caused by mutations in genes that encode the SPASTIN (SPG4), ATLASTIN-1 (SPG3), and REEP1 (SPG31) proteins. Previous reports showed that these proteins bind to one another and shape the tubular endoplasmic reticulum network throughout cells and are also involved in lipid droplet formation and enlargement [34,35]. In addition, recessive forms of HSP genes have been linked to alterations in gene expressions involved in fatty acid metabolism, such as *DDHD1* and *DDHD2* [36,37]. These findings and our experiments with *Spast*-knockdown Neuro 2a lines suggested that altered lipid metabolism in HSP may have elevated *miR-33a* in our SPG4-derived neurons. However, relevance between neurodegeneration and alteration of lipid metabolism has not been clarified yet. Further investigations to connect function of *miR-33* and mechanisms of neurodegenerative diseases including motor neuron diseases are required.

There were several limitations to our study. First, we examined SPG4-derived neurons from only one patient with a splice-site mutation. There are over 40 spastin gene mutations described to date, including missense, nonsense, and deletion mutations. Second, we could only restore neurite length but not branching in the experiments with overexpression of SPAST and LNA anti-*miR-33a* transfection. This may be because of the relatively short duration of observation period. We analyzed 10 days after the transfection in Figure 4 to avoid possible silencing effect of the lentiviral-mediated protein expression. We also measured the neurite length at 48 h after LNA transfection according to the manufacturer's protocol in Figure 5. Third, targeting the *SPAST* 3'-UTR in SPG4 patients through *miR-33a* may up-regulate both normal and mutant *SPAST*. However, it was reported that the truncated mRNA was detected but truncated SPASTIN protein was not detected in brain [38]. Thus, this possibility seems to be low. In addition, it was important to develop a drug delivery system to cross the blood–brain barrier for the treatment of neural diseases by synthetic RNA oligonucleotides.

In summary, we identified that *SPAST*, one of the genes responsible for HSP-SPG4, was a novel target gene of *miR-33* in human. Inhibition of *miR-33a* by LNA normalized the pathological phenotypes such as reduction in neurite length of SPG4-derived cortical neurons. Our findings indicated that *miR-33a* could be a potential therapy for the treatment of SPG4.

Clinical perspectives

- Physiological functions of *miR-33* in humans are still unknown because of a lack of appropriate models.
- We demonstrated for the first time that SPAST is a novel target gene of *miR-33* in human by the generation of *miR-33a/b* deficient human iPSCs.
- *miR-33a* can be a potential therapeutic target for the treatment of HSP-SPG4.

Acknowledgements

The authors would like to express his sincere gratitude to all of his coworkers and collaborators; to Takako Enami for technical assistance; and to Noriko Endo, Ruri Taniguchi, Mikie Iijima, and Makiko Yasui for their valuable administrative support.

Competing interests

The authors declare that there are no competing interests associated with the manuscript.

Funding

This work was supported by the Ministry of Education, Culture, Sports, Science, and Technology (MEXT) and the Japan Society for the Promotion of Science (JSPS) KAKENHI [grants numbers: JP1605297 (to T.K.); JP17H04177, JP17H05599 (to K.O.)]; the Research Project for Practical Applications of Regenerative Medicine from AMED (to H.I.); the Core Center for iPSC Research of Research Center Network for Realization of Regenerative Medicine from AMED (to H.I.); and a visionary research grant (Step) from Takeda Science Foundation (to K.O.). The experimental protocols dealing with human or animal subjects were approved by the institutional review board of each institute.

Author contribution

F.N., I.T., T.H., K.I., H.I., and K.O. designed the project; F.N., I.T., K.I. and K.T. performed experiments; F.N., I.T., T.H., K.I., A.H., O.B., Y.K., T.N., T.N., M.N., H. N., Y.N., Y.I., S.K., M.K., S.T., M.N., S.S., T.K., H.I., and K.O. analyzed and interpreted data; A.H. and H.I. contributed reagents, materials, and analysis tools; Y.I., T.K., and R.K. recruited patients; and F.N., I.T., K.I., H.I., and K.O. prepared the manuscript.

Abbreviations

ANOVA, analysis of variance; CRISPR, clustered regularly interspaced short palindromic repeat; EB, embryoid body; GFP, green fluorescent protein; HSP, hereditary spastic paraplegia; iPSC, induced pluripotent stem cell; IRES, internal ribosome entry site; KO, knockout; LNA, locked nucleic acid; miR, microRNA; miR-C, miR-control; PBS, phosphate-buffered saline; SPAST, spastin protein; SREBF, sterol regulatory element binding factor; SREBP, sterol regulatory element binding protein.

References

- Landgraf, P., Rusu, M., Sheridan, R., Sewer, A., Iovino, N., Aravin, A. et al. (2007) A mammalian microRNA expression atlas based on small RNA library sequencing. *Cell* **129**, 1401–1414, <https://doi.org/10.1016/j.cell.2007.04.040>
- Jovičić, A., Roshan, R., Moison, N., Pradervand, S., Moser, R., Pillao, B. et al. (2013) Comprehensive expression analyses of neural cell-type-specific miRNAs identify new determinants of the specification and maintenance of neuronal phenotypes. *J. Neurosci.* **33**, 5127–5137, <https://doi.org/10.1523/JNEUROSCI.0600-12.2013>
- Horie, T., Ono, K., Horiguchi, M., Nishi, H., Nakamura, T., Nagao, K. et al. (2010) MicroRNA-33 encoded by an intron of sterol regulatory element-binding protein 2 (Srebp2) regulates HLD *in vivo*. *Proc. Natl. Acad. Sci. U.S.A.* **107**, 17321–17326, <https://doi.org/10.1073/pnas.1008499107>
- Rayner, K.J., Suárez, Y., Dávalos, A., Parathath, S., Fitzgerald, M.L., Tamehiro, N. et al. (2010) MiR-33 contributes to the regulation of cholesterol homeostasis. *Science* **328**, 1570–1573, <https://doi.org/10.1126/science.1189862>
- Najafi-Shoushtari, S.H., Kristo, F., Li, Y., Shioda, T., Cohen, D.E., Gerszten, R.E. et al. (2010) MicroRNA-33 and the SREBP host genes cooperate to control cholesterol homeostasis. *Science* **328**, 1566–1569, <https://doi.org/10.1126/science.1189123>
- Marquart, T.J., Allen, R.M., Ory, D.S. and Baldeán, A. (2010) miR-33 links SREBP-2 induction to repression of sterol transporters. *Proc. Natl. Acad. Sci. U.S.A.* **107**, 12228–12232, <https://doi.org/10.1073/pnas.1005191107>
- Errico, A., Ballabio, A. and Rugaelli, E.I. (2002) Spastin, the protein mutated in autosomal dominant hereditary spastic paraplegia, is involved in microtubule dynamics. *Hum. Mol. Genet.* **11**, 153–163, <https://doi.org/10.1093/hmg/11.2.153>
- Evans, K.J., Gomes, E.R., Reisenweber, S.M., Gundersen, G.G. and Lauring, B.P. (2005) Linking axonal degeneration to microtubule remodeling by Spastin-mediated microtubule severing. *J. Cell Biol.* **168**, 599–606, <https://doi.org/10.1083/jcb.200409058>
- Roll-Mecak, A. and Vale, R.D. (2005) The Drosophila homologue of the hereditary spastic paraplegia protein, spastin, severs and disassembles microtubules. *Curr. Biol.* **15**, 650–655, <https://doi.org/10.1016/j.cub.2005.02.029>
- Hazan, J., Fonknechten, N., Mavel, D., Patemotte, C., Samson, D., Artiguenave, F. et al. (1999) Spastin, a new AAA protein, is altered in the most frequent form of autosomal dominant spastic paraplegia. *Nat. Genet.* **23**, 296–303, <https://doi.org/10.1038/15472>
- Bürger, J., Fonknechten, N., Holtzenbein, M., Neumann, L., Bratanoff, E., Hazen, J. et al. (2000) Hereditary spastic paraplegia caused by mutations in the SPG4 gene. *Eur. J. Hum. Genet.* **8**, 771–776, <https://doi.org/10.1038/sj.ejhg.5200528>
- Shoukier, M., Neesen, J., Sauter, S.M., Argyriou, L., Doerwald, N., Pantakani, D.V. et al. (2009) Expansion of mutation spectrum, determination of mutation cluster regions and predictive structural classification of SPAST mutations in hereditary spastic paraplegia. *Eur. J. Hum. Genet.* **17**, 187–194, <https://doi.org/10.1038/ejhg.2008.147>
- Kim, Y.K., Wee, G., Park, J., Kim, J., Baek, D., Kim, J.S. et al. (2013) TALEN-based knockout library for human microRNAs. *Nat. Struct. Mol. Biol.* **20**, 1458–1464, <https://doi.org/10.1038/nsmb.2701>
- Change, H., Yi, B., Ma, R., Zhang, X., Zhao, H. and Xi, Y. (2016) CRISPR/cas9, a novel genomic tool to knockdown microRNA *in vitro* and *in vivo*. *Sci. Rep.* **6**, 22312, <https://doi.org/10.1038/srep22312>
- Claudiani, P., Rinano, E., Errico, A., Andolfi, G. and Rugarli, E.I. (2005) Spastin subcellular localization is regulated through usage of different translation start sites and active export from the nucleus. *Exp. Cell Res.* **309**, 358–369, <https://doi.org/10.1016/j.yexcr.2005.06.009>
- Solowska, J.M., Morfini, G., Falnikar, A., Himes, B.T., Brady, S.T., Huang, D. et al. (2008) Quantitative and functional analyses of spastin in the nervous system: implications for hereditary spastic paraplegia. *J. Neurosci.* **28**, 2147–2157, <https://doi.org/10.1523/JNEUROSCI.3159-07.2008>
- Solowska, J.M., Garbern, J.Y. and Baas, P.W. (2010) Evaluation of loss-of-function as an explanation for SPG4-based hereditary spastic paraplegia. *Human Mol. Genet.* **19**, 2767–2779, <https://doi.org/10.1093/hmg/ddq177>
- Svenson, I.K., Ashley-Koch, A.E., Gaskell, P.C., Riney, T.J., Cumming, W.J., Kingston, H.M. et al. (2001) Identification and expression analysis of spastin gene mutations in hereditary spastic paraplegia. *Am. J. Hum. Genet.* **68**, 1077–1085, <https://doi.org/10.1086/320111>
- Kondo, T., Asai, M., Tsukita, K., Kutoku, Y., Ohsawa, Y., Sunada, Y. et al. (2013) Modeling Alzheimer's disease with iPSCs reveals stress phenotypes associated with intracellular A β and differential drug responsiveness. *Cell Stem Cell* **12**, 487–496, <https://doi.org/10.1016/j.stem.2013.01.009>
- Havlicek, S., Kohl, Z., Mishra, H.K., Prots, I., Eberhardt, E., Denguir, N. et al. (2014) Gene dosage-dependent rescue of HSP neurite defects in SPG4 patients' neurons. *Hum. Mol. Genet.* **23**, 2527–2541, <https://doi.org/10.1093/hmg/ddt644>
- Horie, T., Nishino, T., Baba, O., Kuwabara, Y., Nakao, T., Nishiga, M. et al. (2013) MicroRNA-33 regulates sterol regulatory element-binding protein 1 expression in mice. *Nat. Commun.* **4**, 2883, <https://doi.org/10.1038/ncomms3883>

- 22 Nakao, T., Horie, T., Baba, O., Nishiga, M., Nishino, T., Izuhara, Y. et al. (2017) Genetic ablation of microRNA-33 attenuates inflammation and abdominal aortic aneurysm formation via several anti-inflammatory pathways. *Arterioscler. Thromb. Vasc. Biol.* **37**, 2161–2170, <https://doi.org/10.1161/ATVBAHA.117.309768>
- 23 Nishiga, M., Horie, T., Kuwabara, Y., Nagao, K., Baba, O., Nakao, T. et al. (2017) MicroRNA-33 controls adaptive fibrotic response in the remodeling heart by preserving lipid raft cholesterol. *Circ. Res.* **120**, 835–847, <https://doi.org/10.1161/CIRCRESAHA.116.309528>
- 24 Golde, T.E., Borchelt, D.R., Glasson, B.I. and Lewis, J. (2013) Thinking laterally about neurodegenerative proteinopathies. *J. Clin. Invest.* **123**, 1847–1855, <https://doi.org/10.1172/JCI66029>
- 25 Denton, K.R., Lei, L., Grenier, J., Rodionov, V., Blackstone, C. and Li, X.J. (2014) Loss of spastin function results in disease-specific axonal defects in human pluripotent stem cell-based models of hereditary spastic paraplegia. *Stem Cells* **32**, 414–423, <https://doi.org/10.1002/stem.1569>
- 26 Solowska, J.M. and Baas, P.W. (2015) Hereditary spastic paraplegia SPG4: what is known and not known about the disease. *Brain* **138**, 2471–2484, <https://doi.org/10.1093/brain/awv178>
- 27 Stein, C.A. and Castanotto, D. (2017) FDA-approved oligonucleotide therapies in 2017. *Mol. Ther.* **25**, 1069–1075, <https://doi.org/10.1016/j.ymthe.2017.03.023>
- 28 Lin, Y., Liu, A.Y., Fan, C., Zheng, H., Li, Y., Zhang, C. et al. (2015) MicroRNA-33b inhibits breast cancer metastasis by targeting HMGA2, SALL4 and Twist1. *Sci. Rep.* **5**, 9995, <https://doi.org/10.1038/srep09995>
- 29 Zhang, C., Zhang, Y., Ding, W., Lin, Y., Huang, Z. and Luo, Q. (2015) MiR-33a suppresses breast cancer cell proliferation and metastasis by targeting ADAM9 and ROS1. *Protein Cell* **6**, 881–889, <https://doi.org/10.1007/s13238-015-0223-8>
- 30 Hébert, S.S., Horré, K., Nicolai, A.S., Papadopoulou, A.S., Mandemakers, W., Silahtaroglu, A.N. et al. (2008) Loss of microRNA cluster miR-29a/b-1 in sporadic Alzheimer's disease correlates with increased BACE1/ beta-secretase expression. *Proc. Natl. Acad. Sci. U.S.A.* **105**, 6415–6420, <https://doi.org/10.1073/pnas.0710263105>
- 31 Lukiw, W.J. (2007) Micro-RNA speciation in fetal, adult and Alzheimer's disease hippocampus. *Neuroreport* **18**, 297–300, <https://doi.org/10.1097/WNR.0b013e3280148e8b>
- 32 Kim, J., Yoon, H., Horie, T., Burchett, J.M., Restivo, J.L., Rotllan, N. et al. (2015) microRNA-33 regulates apoE lipidation and amyloid- β metabolism in the brain. *J. Neurosci.* **35**, 14714–14726, <https://doi.org/10.1523/JNEUROSCI.2053-15.2015>
- 33 Kim, J., Inoue, K., Ishii, J., Vanti, W.B., Voronov, S.V., Murchison, E. et al. (2007) A MicroRNA feedback circuit in midbrain dopamine neurons. *Science* **317**, 1220–1224, <https://doi.org/10.1126/science.1140481>
- 34 Renvoisé, B., Malone, B., Falgairolle, M., Munasinghe, J., Stadler, J., Sibilla, C. et al. (2016) Reep1 null mice reveal a converging role for hereditary spastic paraplegia proteins in lipid droplet regulation. *Human Mol. Genet.* **25**, 5111–5125
- 35 Paradopoulos, C., Orso, G., Mancuso, G., Herholz, M., Gumeni, S., Tadepalle, N. et al. (2015) Spastin binds to lipid droplets and affects lipid metabolism. *PLoS Genet.* **11**, e1005149, <https://doi.org/10.1371/journal.pgen.1005149>
- 36 Tesson, C., Nawara, M., Salih, M.A., Rossignol, R., Zaki, M.S., AL Balwi, M. et al. (2012) Alteration of fatty-acid-metabolizing enzymes affects mitochondrial form and function in hereditary spastic paraplegia. *Am. J. Hum. Genet.* **91**, 1051–1064, <https://doi.org/10.1016/j.ajhg.2012.11.001>
- 37 Schuurs-Hoeijmakers, J.H., Geraghty, M.T., Kamsteeg, E.J., Ben-Salem, S., de Bot, S.T., Nijhof, B. et al. (2012) Mutations in DDHD2, encoding an intracellular phospholipase A(1), cause a recessive form of complex hereditary paraplegia. *Am. J. Hum. Genet.* **91**, 1073–1081, <https://doi.org/10.1016/j.ajhg.2012.10.017>
- 38 Tarrade, A., Fassier, C., Courageot, S., Charvin, D., Vitte, J., Peris, L. et al. (2006) A mutation of spastin is responsible for swellings and impairment of transport in a region of axon characterized by changes in microtubule composition. *Hum. Mol. Genet.* **15**, 3544–3558, <https://doi.org/10.1093/hmg/ddl431>
- 39 Okita, K., Yamakawa, T., Matsumura, Y., Sato, Y., Amano, N., Watanabe, A. et al. (2013) An efficient nonviral method to generate integration-free human-induced pluripotent stem cells from cord blood and peripheral blood cells. *Stem Cells* **31**, 458–466, <https://doi.org/10.1002/stem.1293>
- 40 Horie, T., Ono, K., Nishi, H., Nagao, K., Kinoshita, M., Wanatabe, S. et al. (2010) Acute doxorubicin cardiotoxicity is associated with miR-146a-induced inhibition of the neuregulin-ErbB pathway. *Cardiovasc. Res.* **87**, 656–664, <https://doi.org/10.1093/cvr/cvq148>
- 41 Nishi, H., Ono, K., Iwanaga, Y., Horie, T., Nagao, K., Takemura, G. et al. (2010) MicroRNA-15b modulates cellular ATP levels and degenerates mitochondria via Arl2 in neonatal rat cardiac myocytes. *J. Biol. Chem.* **285**, 4920–4930, <https://doi.org/10.1074/jbc.M109.082610>